

# Integration of individual TiO<sub>2</sub> nanotube on the chip: Nanodevice for hydrogen sensing

Mihail Enachi<sup>\*,1</sup>, Oleg Lupan<sup>\*,\*\*2</sup>, Tudor Braniste<sup>1</sup>, Andrei Sarua<sup>3</sup>, Lee Chow<sup>4</sup>, Yogendra K. Mishra<sup>2</sup>, Dawit Gedamu<sup>2</sup>, Rainer Adelung<sup>2</sup>, and Ion Tiginyanu<sup>1,5</sup>

<sup>1</sup> National Center for Materials Study and Testing, Technical University of Moldova, 2004 Chisinau, Republic of Moldova

<sup>2</sup> Functional Nanomaterials, Institute for Materials Science, Christian Albrechts University of Kiel, 24143 Kiel, Germany

<sup>3</sup> H.H. Wills Physics Laboratory, University of Bristol, BS8 1TL Bristol, UK

<sup>4</sup> Department of Physics, University of Central Florida, Orlando, FL 32816-2385, USA

<sup>5</sup> Institute of Electronic Engineering and Nanotechnologies, Academy of Sciences of Moldova, 2028 Chisinau, Republic of Moldova

Received 28 December 2014, revised 19 February 2015, accepted 19 February 2015

Published online 24 February 2015

**Keywords** TiO<sub>2</sub>, nanotubes, hydrogen, gas sensors, anatase, rutile

\* Corresponding authors: e-mail [enachimihai@mail.utm.md](mailto:enachimihai@mail.utm.md), Phone: +373 22 509 920, Fax: +373 22 509 920; e-mail [ollu@tf.uni-kiel.de](mailto:ollu@tf.uni-kiel.de)

\*\* On leave from Department of Microelectronics and Biomedical Engineering, Technical University of Moldova, 168 Stefan cel Mare Blvd., 2004 Chisinau, Republic of Moldova.

Titania (TiO<sub>2</sub>) exists in several phases possessing different physical properties. In view of this fact, we report on three types of hydrogen sensors based on individual TiO<sub>2</sub> nanotubes (NTs) with three different structures consisting of amorphous, anatase or anatase/rutile mixed phases. Different phases of the NTs were produced by controlling the temperature of post-anodization thermal treatment. Integration of individual TiO<sub>2</sub> nanotubes on the chip was performed by employing metal deposition function in the focused ion beam (FIB/SEM) instrument. Gas response was studied for devices made from an as-grown individual nanotube with an amor-

phous structure, as well as from thermally annealed individual nanotubes exhibiting anatase crystalline phase or anatase/rutile heterogeneous structure. Based on electrical measurements using two Pt complex contacts deposited on a single TiO<sub>2</sub> nanotube, we show that an individual NT with an anatase/rutile crystal structure annealed at 650 °C has a higher gas response to hydrogen at room temperature than samples annealed at 450 °C and as-grown. The obtained results demonstrate that the structural properties of the TiO<sub>2</sub> NTs make them a viable new gas sensing nanomaterial at room temperature.

© 2015 WILEY-VCH Verlag GmbH & Co. KGaA, Weinheim

**1 Introduction** The high interest in titanium dioxide or titania has been stimulated for decades by a myriad of applications of this versatile material such as heterogeneous catalysis, photocatalysis, solar cells, chemical sensors, corrosion-protective coatings, biomedicine etc. [1–4]. Over the last few years, increased attention has been paid to the study of nanostructured TiO<sub>2</sub> layers and membranes fabricated by anodic oxidation of pure titanium foils [5]. Recently we observed, for example, that anodic oxidation of Ti foils at temperatures below 0 °C leads to the formation of closely packed TiO<sub>2</sub> nanotubes distributed in a two-dimensional quasi-ordered fashion [6]. These findings open up new perspectives to the applications of TiO<sub>2</sub> nanotubular structures in the design and fabrication of novel photonic elements [7]. Among other applications, increas-

ing interest has also been devoted to gas sensing properties of titania. TiO<sub>2</sub> based gas sensors were made by various processes such as thermal evaporation of TiO<sub>2</sub> powder [8], electrochemical deposition [9], anodization of Ti sheets in water based solutions containing fluoride ions [10], or organic electrolytes [11], etc. Sensing properties of TiO<sub>2</sub> have been investigated in film sensors [9], dots or TiO<sub>2</sub> nanotubular arrays [10]. Hydrogen gas sensors on undoped TiO<sub>2</sub> [12] and doped TiO<sub>2</sub> nanostructures with different dopants such as Nb [13], Eu, Yb, Pt [14], C or mixture of TiO<sub>2</sub> and other nanocompounds such as SnO<sub>2</sub> were previously reported by different groups. Vertically aligned and ordered TiO<sub>2</sub> NT arrays have been investigated as hydrogen sensors due to their change of electrical resistance in the presence of hydrogen gas [10]. It is well known that the

working mechanism of chemical sensors originates from surface phenomena, and therefore nanostructures, especially an individual TiO<sub>2</sub> NT, can offer extra advantages for chemical nanosensors.

To the best of our knowledge, there are no reports in the literature on gas sensors fabricated on individual TiO<sub>2</sub> nanotube. Here, we report for the first time on hydrogen nanosensors developed by using an individual TiO<sub>2</sub> nanotube integrated on the chip and demonstrate a higher gas response to hydrogen from samples annealed at 650 °C than samples annealed at 450 °C and as-grown.

**2 Experimental details** TiO<sub>2</sub> nanotubes were obtained by electrochemical anodization of Ti foil (from Sigma-Aldrich) with thickness of 0.25 mm and purity of 99.7%. Prior to the anodic oxidation, the sample was degreased in an ultrasonic bath using acetone and isopropyl alcohol, followed by rinsing in deionized water, and then dried under a nitrogen stream. The solution used in anodization experiments is described in a previous work [15]. The anodization was performed at room temperature, for 2 h and with a voltage of 120 V applied to the sample. This allowed us to obtain TiO<sub>2</sub> nanotubular membranes with the thickness of 20 μm (~ nanotube length) and the inner diameter of the tubes of about 80–120 nm.

The electrochemical anodization process was performed in a standard electrochemical cell based on three electrodes, with Ag/AgCl (1 M KCl) as reference electrode. The potential between the measuring electrode and the reference one as well as the anodic oxidation current were measured by a Keithley 2400 digital multimeter.

The morphology of specimens was investigated by scanning electron microscope Ultra 55 Zeiss FEG (10 kV). A WITec Raman equipment was used for Raman scattering characterization of the nanotubes. Excitation of samples was provided by a 532 nm line from a frequency doubled Nd:YAG laser at an output power of 10 mW [16].

The separation of individual nanotubes from the entire membrane has been performed using an ultrasound bath. The membrane was placed in ethanol and then subjected to ultrasonic treatment for 15 s which resulted in a solution containing dispersed TiO<sub>2</sub> NTs. Micro-drop of the solution containing TiO<sub>2</sub> NTs was transferred using a pipette on a Si/SiO<sub>2</sub> substrate, afterwards transferred to the chip with pre-patterned Au metal contacts. The nanotubes were placed between the contacts using previously developed technique by Lupan et al. [16–18].

Focused ion beam metal deposition function of FIB-SEM instrument Dualbeam Helios Nanolab (FEI) (10 kV, 0.34 nA) [16] was applied to deposit two rigid Pt complex contacts on each individual TiO<sub>2</sub> nanotube. Three different types of titania NTs, namely as-grown, annealed at 450 °C, and annealed at 650 °C were used as raw material for sensor fabrication. The gas responses of fabricated nanosensors were tested in the presence of H<sub>2</sub> at room temperature as reported previously [17, 18]. The H<sub>2</sub> gas pulses of 1000 ppm were applied in experiments as before [16–18].

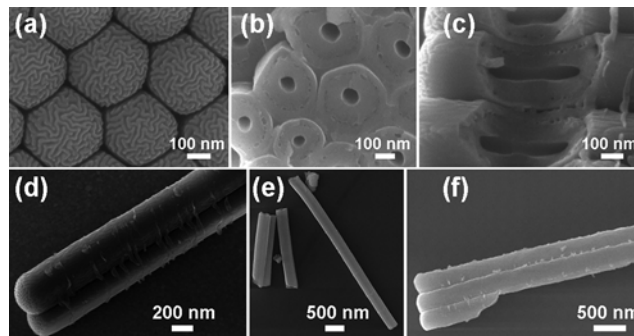


**Figure 1** SEM images taken from a TiO<sub>2</sub> nanotubular membrane: (a) bottom view, (b) top view, (c) longitudinal section taken from a cluster of nanotubes showing a tubular morphology along its length. (d, e, f) As-grown, annealed respectively at 450 °C and 650 °C in air and separated from the membrane.

**3 Results and discussion** The SEM image of the bottom side of the TiO<sub>2</sub> nanotubular membrane is presented in Fig. 1a, and the top surface of the TiO<sub>2</sub> membrane is shown in Fig. 1b. Interestingly, the bottom surface is not smooth and is crossed by numerous convolutions, unique for each tube (Fig. 1a). These features represent a 'fingerprint' of the tube, providing a possibility of identifying each tube individually. The obtained nanotubes exhibit a double-wall structure (Fig. 1c), which is in agreement with previous observations [19]. Figure 1d shows a pair of as-grown NTs detached from the titania membrane by the technique described above. Figure 1e and f show SEM images of the NT samples annealed in air at 450 °C and 650 °C, respectively.

Post-anodization thermal treatment at 450 °C and 650 °C in air was applied to modify the structure of titania NTs [20]. Post-growth treatment and the resulting crystal phases have a significant impact on the electronic, mechanical, optical, and chemical properties of the TiO<sub>2</sub> NTs [20].

The analysis of micro-Raman spectra shown in Fig. 2a suggests that as-prepared TiO<sub>2</sub> nanotubes are amorphous (red curve), while those annealed at 450 °C exhibit anatase (An) crystalline structure (black curve). The peaks at 399, 514 and 639 cm<sup>-1</sup> correspond to anatase phase [21]. Along

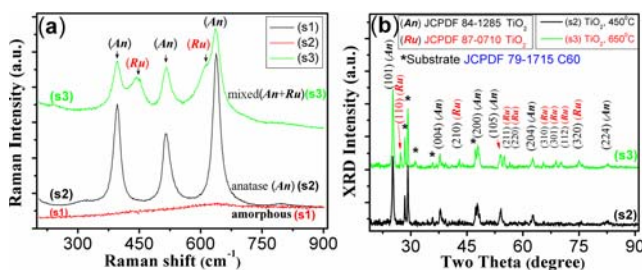


**Figure 2** (a) Micro-Raman scattering spectra taken from initial individual TiO<sub>2</sub> nanotube (red curve), TiO<sub>2</sub> nanotube annealed at 450 °C (black curve – An) and 650 °C (green curve – An + Ru). (b) The X-ray diffraction patterns of the product from TiO<sub>2</sub> NTs (s2, annealed at 450 °C and s3 annealed at 650 °C).

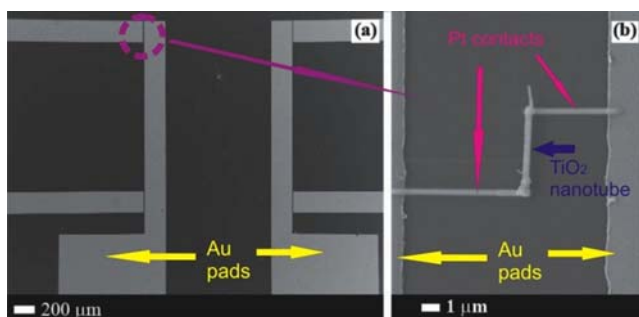


**Figure 3** SEM image of (a) a chip fabricated on Si/SiO<sub>2</sub> substrate with Au electrical contacts, (b) a gas sensor made from a single nanotube with amorphous structure.

with these three peaks, two additional peaks at 612 cm<sup>-1</sup> and 447 cm<sup>-1</sup> are observed in Raman spectrum taken from samples annealed at 650 °C, see Fig. 2a (green curve), which are inherent to the rutile (*Ru*) phase of TiO<sub>2</sub> [22]. Note that rutile is generally considered to be the thermodynamically most stable phase of TiO<sub>2</sub>. The XRD data presented in Fig. 2b confirms micro-Raman observations on TiO<sub>2</sub> NTs.

Figure 3 represents a SEM image taken from a chip fabricated on a Si/SiO<sub>2</sub> substrate (Fig. 3a) with gas sensor based on a single TiO<sub>2</sub> nanotube with amorphous structure placed between electrical contacts (Fig. 3b). Similar devices on individual NTs were made from all three types of NTs (not shown here to avoid repetition). The NT length in device was about 4 μm in all cases.

The current–voltage (*I*–*V*) dependence taken from three types of sensors under consideration shows a similar behavior in the range from –10 V to +10 V as illustrated in Fig. 4a. In all types of nanosensors, the current increased when the sensors were exposed to H<sub>2</sub> gas and recovered to the initial value when the H<sub>2</sub> gas atmosphere was replaced by air. Note that the sensor response was quite stable over many cycles of exposure to H<sub>2</sub> gas. However, as one can see in Fig. 4(b–d), there are notable differences in the responses to the gas among sensors based on nanotubes with three different crystalline structures consisting of amorphous, anatase or mixed anatase/rutile phases. In particular, when a gas pulse is applied, the current increases up to a maximum value more slowly in the sensor based on amorphous nanotube (tens of seconds) than it does in nanosensors with anatase crystal structure (rise time constant  $\tau_{r1} = \tau_{r2} \sim 1.37$  s) or mixed anatase/rutile crystal structure ( $\tau_{r1} = \tau_{r2} \sim 0.7$  s). Besides, in the case of single nanotube sensor with amorphous or pure anatase structure, two distinctive regions of the relaxation process are observed after exposure to the gas pulses (Fig. 4b, c). For the amorphous TiO<sub>2</sub> NT-based sensor structure, these two slopes of recovery curves (Fig. 4b) can be characterized as follows: during first 30–40 s the current drops by 90% of the maximum value, followed by a much slower current decrease (Fig. 4b). In the case of the sensor with anatase crystal structure (Fig. 4c) there is a relatively rapid decrease of the current during initial period (decay time constant  $\tau_d \sim 3$  s)

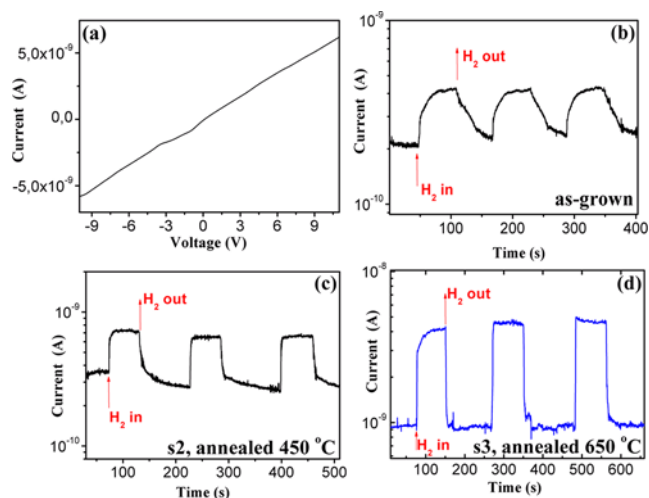


**Figure 4** (a) Current–voltage characteristics of the device. Dynamic changes in the electrical current in response to hydrogen gas for a single TiO<sub>2</sub> nanotubular sensor with: (b) amorphous, (c) anatase and (d) mixed anatase/rutile structures, measured at 300 K under applied voltage of +10 V.

after H<sub>2</sub> gas was turned off, followed by a rather slow decrease. In both cases current reaches a value very close to its original baseline value after exposure to air for about 180 s. However, the NT sensor containing anatase/rutile phase shows a much faster response ( $\tau_{r1} = \tau_{r2} \sim 0.7$  s) and recovery times ( $\tau_{d1} = \tau_{d2} \sim 0.9$  s) in comparison with previous two types of nanosensors. In this case, to find time constants, least square fittings were performed with equations  $I(t) = I_0 + A_1 e^{t/\tau_{r1}} + A_2 e^{t/\tau_{r2}}$  and  $I(t) = I_0 + A_3 e^{-t/\tau_{d1}} + A_4 e^{-t/\tau_{d2}}$ , where  $I_0$  is dark current,  $A_1$ ,  $A_2$ ,  $A_3$  and  $A_4$  are positive constants,  $\tau_{r1}$ ,  $\tau_{r2}$  and  $\tau_{d1}$ ,  $\tau_{d2}$  are time constants for rising and decaying current, respectively.

The fundamental mechanisms that cause resistance changes are still controversial [17, 18, 23], but essentially trapping/releasing of electrons at adsorbed O<sub>2</sub> and H<sub>2</sub> and band bending induced by these charged molecules are mainly responsible for a change in resistance. When NTs are placed in atmosphere, the oxygen from air is adsorbed as follows [16, 24]: (O<sub>2(gas)</sub> → O<sub>2(ads)</sub>; O<sub>2(ads)</sub> + e<sup>-</sup> ↔ O<sub>2(ads)</sub><sup>-</sup>; O<sub>2(ads)</sub><sup>-</sup> + e<sup>-</sup> ↔ 2O<sub>(ads)</sub><sup>-</sup>; O<sub>(ads)</sub><sup>-</sup> + e<sup>-</sup> ↔ O<sub>(ads)</sub><sup>2-</sup>) on the nanotube surface by capturing a free electron from nanomaterial, leading to an enhanced base resistance [16–18]. An electron-depletion layer is formed on the NT surface. It is important to point out, that the types of chemisorbed oxygen species (O<sub>2</sub><sup>-</sup>, O<sup>-</sup> and O<sup>2-</sup>) depend strongly on temperature [16, 17, 23, 24]. When the sensor is exposed to a reducing gas (H<sub>2</sub>), it removes these adsorbed ionized oxygen species (e.g. O<sub>2</sub><sup>-</sup>, O<sup>-</sup> and O<sup>2-</sup>) by reversible chemisorptions (H<sub>2</sub> + 1/2O<sub>2(ads)</sub><sup>-</sup> → H<sub>2</sub>O<sub>(gas)</sub> + e<sup>-</sup>), thus reducing the electrical resistance due to releasing of the electrons in the NT [12, 17, 18]. It is important to mention other mechanisms responsible for gas sensing of TiO<sub>2</sub>. Previous results indicate that the gas sensing response properties of TiO<sub>2</sub> based

sensors might be attributed to the interaction between target gas and material bulk defects [25].

Our data show that the best performance was found in the sensors made from NTs annealed at 650 °C, i.e., in the devices with mixed anatase/rutile crystal structure. The observed response time for these sensors is about 0.7–0.9 seconds (Fig. 4d), this value being characteristic for both cases of current increase when the sensor is exposed to the H<sub>2</sub> gas and current relaxation after exposure to the gas pulse. Therefore, it can be suggested that mixing of two crystal phases of TiO<sub>2</sub> has significant influence on the gas sensing performance of the titania NTs. Also, it is important to mention that such sensor structures exhibit a reliable operation to H<sub>2</sub> gas in air, while previous reports showed H<sub>2</sub> sensing in a N<sub>2</sub> gas environment [10, 12]. A synergistic effect between anatase and rutile TiO<sub>2</sub> is known for other applications too [26].

An individual TiO<sub>2</sub> nanotube represents in our third case a heterogeneous nanocrystalline material consisting of anatase and rutile phases. One can expect that there is a potential barrier between them, which the electrons should overcome, and this may be of importance since the operation of nanocrystalline sensors is usually based on resistance modulation (decrease or increase of potential barriers due to interaction with the gas medium). So, one can speculate that the increased response and faster response/recovery in the third case is caused by the nanotube material. It may result in the occurrence along the tube of potential barriers which are effectively modulated by the gas adsorption/desorption.

**4 Conclusions** We demonstrated a novel type of hydrogen sensors based on an individual TiO<sub>2</sub> nanotube fabricated by anodic etching of Ti foils, subsequent sonication and its direct integration on the chip. Post-anodization thermal treatment at 450 °C and 650 °C in air was applied to control the crystalline structure of titania NTs. As a result of a comparative analysis of sensors characteristics based on amorphous (as-grown), anatase (annealed at 450 °C) and mixed anatase/rutile (annealed at 650 °C) structures, we found that single nanotube with anatase/rutile structure shows a faster response of ~1 s to hydrogen gas in air at room temperature. Along with this, the response for such sensor structures is 3 times larger than for amorphous ones and the recovery time is about 1 s. The obtained results prove that individual TiO<sub>2</sub> nanotubes represent a promising platform for gas nanosensor applications, especially when low-cost, small size and fast response should be secured.

**Acknowledgements** This work was partially financially supported by the Academy of Sciences of Moldova under the Grant no. 11.817.05.19A. Stefan Rehders is acknowledged for technical support. Dr. Lupan gratefully acknowledges the Alexander von Humboldt Foundation for the research fellowship for experienced researchers at the Christian Albrechts University of Kiel, Germany.

## References

- [1] K. Hashimoto, H. Irie, and A. Fujishima, *Jpn. J. Appl. Phys.* **44**, 8269–8285 (2005).
- [2] J. Wang and Z. Lin, *Chem. Asian J.* **7**, 2754–2762 (2012).
- [3] K. O. Awitor, A. Rivaton, J.-L. Gardette, A. J. Down, and M. B. Johnson, *Thin Solid Films* **516**, 2286–2291 (2008).
- [4] C. Perez-Jorge, A. Conde, M. A. Arenas, R. Perez-Tanoira, E. Matykina, J. J. de Damborenea, E. Gomez-Barrena, and J. Esteban, *J. Biomed. Mater. Res. A* **100**, 1696–1705 (2012).
- [5] K. Shankar, G. K. Mor, H. E. Prakasam, S. Yoriya, and M. Paulose, *Nanotechnology* **18**, 065707 (2007).
- [6] M. Enachi, M. Stevens-Kalceff, I. Tiginyanu, and V. Ursaki, *Mater. Lett.* **64**, 2155–2158 (2010).
- [7] V. V. Sergentu, I. M. Tiginyanu, V. V. Ursaki, M. Enachi, S. P. Albu, and P. Schmuki, *Phys. Status Solidi RRL* **2**, 242–244 (2008).
- [8] D. Manno, G. Micocci, R. Rella, A. Serra, A. Taurino, and A. Tepore, *J. Appl. Phys.* **82**, 54–59 (1997).
- [9] D. Chu, A. Younis, and S. Li, *J. Phys. D: Appl. Phys.* **45**, 355306 (2012).
- [10] O. K. Varghese, D. Gong, M. Paulose, K. G. Ong, and C. A. Grimes, *Sens. Actuators B* **93**, 338–344 (2003).
- [11] H. F. Lu, F. Li, G. Liu, Z. G. Chen, D. W. Wang, H. T. Fang, G. Q. Lu, Z. H. Jiang, and H. M. Cheng, *Nanotechnology* **19**, 405504 (2008).
- [12] E. Sennik, Z. Colak, N. Kilinc, and Z. Z. Ozturk, *Int. J. Hydrogen Energy* **35**, 4420–4427 (2010).
- [13] H. Liu, D. Ding, C. Ning, and Z. Li, *Nanotechnology* **23**, 015502 (2012).
- [14] G. S. Aluri, A. Motayed, A. V. Davydov, V. P. Oleshko, K. A. Bertness, N. A. Sanford, and R. V. Mulপুরi, *Nanotechnology* **23**, 175501 (2012).
- [15] M. Enachi, I. Tiginyanu, V. Sprincean, and V. Ursaki, *Phys. Status Solidi RRL* **4**, 100–102 (2010).
- [16] O. Lupan, V. Cretu, M. Deng, D. Gedamu, I. Paulowicz, S. Kaps, Y. K. Mishra, O. Polonskyi, C. Zamponi, L. Kienle, V. Trofim, I. Tiginyanu, and R. Adelung, *J. Phys. Chem. C* **118**, 15068–15078 (2014).
- [17] O. Lupan, V. V. Ursaki, G. Chai, L. Chow, G. A. Emelchenko, I. M. Tiginyanu, A. N. Gruzintsev, and A. N. Redkin, *Sens. Actuators B* **144**, 56–66 (2010).
- [18] L. Chow, O. Lupan, and G. Chai, *Phys. Status Solidi B* **247**, 1628–1632 (2010).
- [19] S. P. Albu, A. Ghicov, S. Aldabergenova, P. Drechsel, D. LeClere, G. E. Thompson, J. M. Macak, and P. Schmuki, *Adv. Mater.* **20**, 4135–4139 (2008).
- [20] P. Roy, S. Berger, and P. Schmuki, *Angew. Chem. Int. Edit.* **50**, 2904–2939 (2011).
- [21] T. Ohsaka, F. Izumi, and Y. Fujiki, *J. Raman Spectroscopy* **7**, 321–324 (1978).
- [22] S. P. S. Porto, P. A. Fleury, and T. C. Damen, *Phys. Rev.* **154**, 522 (1966).
- [23] Y. Jun, J. H. Park, and M. G. Kang, *Chem. Commun.* **48**, 6456–6471 (2012).
- [24] Z. H. Jing, *Mater. Sci. Eng. A* **441**, 176–180 (2006).
- [25] Y. Shimizu and M. Egashira, *MRS Bull.* **24**, 18–24 (1999).
- [26] G. Li, C. P. Richter, R. L. Milot, and L. Cai, *Dalton Trans.* **45**, 10078–10085 (2009).